here should be suitable for the surface coating described the later section owing to their high dispersibility in liquid media and high thermal and chemical stability.

Starting HAp particles with low crystallinity were prepared by a modified emulsion system at 25°C. The resulting product was centrifugally washed and redispersed in water (solid content: 5 wt%). In order to intersperse $Ca(OH)_2$ -- an anti-sintering agent -- between the particles, the HAp aqueous dispersion was added into a saturated aqueous $Ca(OH)_2$ solution (0.17 wt%), and the mixture was dried under reduced pressure at 40°C. The resultant HAp/$Ca(OH)_2$ (1/1, w/w) mixture was calcined at 800°C for 1 h in air (heating rate: 10°C/min). After calcination, the mixture was centrifugally washed with water to remove the $Ca(OH)_2$. As a control, HAp was calcined using the same procedure without adding $Ca(OH)_2$.

The sizes of the crystals dispersed in ethanol measured by dynamic light scattering were quite different between the two kinds of the calcined HAp with and without $Ca(OH)_2$ as shown in **Fig. 1**. In the case of calcination without $Ca(OH)_2$ shown as the solid columns, the mean size of the HAp crystals dispersed in HAp crystals were dispersed as agglomerates consisting of sintered polycrystals whose mean size indicated about 600 nm. On the other hand, calcining with the anti-sintering agent, the mean size of the crystals was much smaller than that of without the agent. The average size of the HAp nanoparticles shows about 80 nm. The results indicate that the sintering among HAp nanocrystals could be avoided by calcination with $Ca(OH)_2$ interposed among the crystals, followed by removing of $Ca(OH)_2$ after calcination. It was clear that the HAp nanoparticles were scattered by a single particle on a SEM mount.

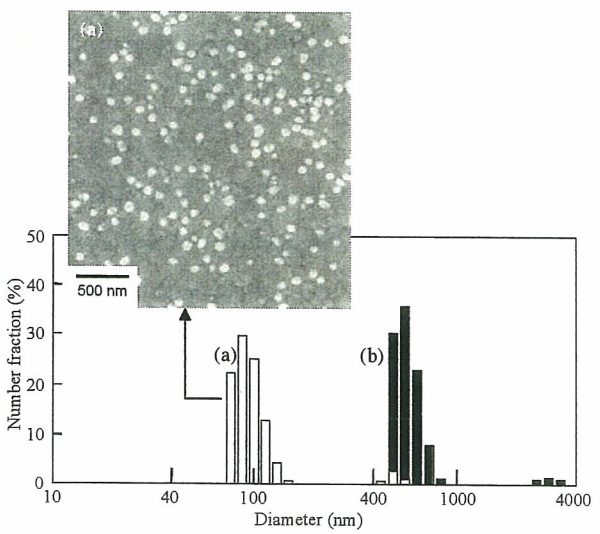

Fig. 1 Size distributions of HAp particles calcined at 800°C for 1 h with (a) and without (b) an anti-sintering agent, The size distribution was measured in ethanol as a medium by using dynamic light scattering.

Nano-HAp coating by chemical bonding

Graft-polymerization with γ-methacryloxyethyl trimethoxysilane(MPTS) monmer having an alkoxysilyl group on SF fibers with 100 μm of length was conducted by free radical initiation. After the HAp particles were suspended in a toluene/methanol (9/1) mixture solvent, a poly(MPTS)-grafted SF was soaked in the suspended solution for 1h at room temperature to be adsorbed on the SF. The SF adsorbed with the HAp particles was washed by stirring in methanol and filtered by a filter with a 5-μm cut-off point to remove unreacted HAp particles. The fibers adsorbed with HAp were heated at 120 °C for 2h in vacuum at 1mmHg for a reaction between the HAp surface and the alkoxysilyl groups of the graft polymers. The composite was washed by using an ultrasonic generator for 3 min (output: 20 kHz and 35W) to remove excess adsorbed HAp particles attached to ones in ethanol. Finally, the composite was washed in a great amount of distilled water for 1 day to remove the residual organic solvents used in the synthetic process. **Fig. 2** shows an SEM photograph of the HAp-coated SF fiber with covalent bonding. A fiber cut approximately 100 μm in length was more effective for the coating than that of a fabric-form. The HAp particles separated and slightly aggregated into several crystals under SEM observation. Generally, aggregation is easy because the HAp mono-particle has an a-plane with a cationic charge and a c-plane with an anionic charge in a mono-crystal. Our high-dispersed HAp nano-crystals were suitable for preparation of mono-layer-like nano-HAp coating.

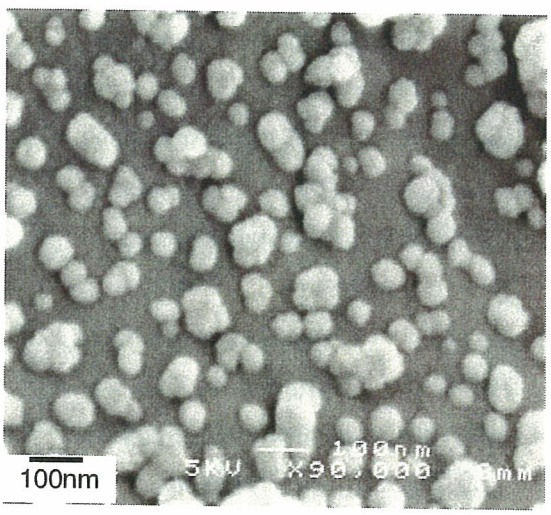

Fig. 2 SEM image of surface of HAp-coated SF by covalent linkage.

Cell Interaction

To evaluate the cell adhesiveness on the HAp-coated silk fibroin (SF), the morphologies of L929 fibroblast cells incubated on sample fabrics were observed by

SEM. **Fig. 3** shows SEM observations of the surfaces of sample fabrics --- gelatin-coated glass as a positive control (a), untreated SF (b), hydrolyzed poly(MPTS)-grafted SF (c) and HAp-coated SF (d) --- incubated with L929 cells for 24 h. The cells hardly adhered on the hydrolyzed poly(MPTS)-grafted SF as well as the untreated SF in **Fig. 3 (b, c)**. Although it has been known that the initial cell adhesion on intact SF is actually not good, the reason has not been thoroughly manifested. It is presumed to depend on high surface wettability due to containing many hydrophilic amino acid residues[17] --- the hydroxyl group: Ser 10.63 mol%, Tyr 4.97 mol%, Thr 0.89 mol%; the carboxyl group: Asp 1.65 mol%, Glu 1.21 mol%; the amino groups: Lys 0.33 mol%, His 0.18 mol%, Arg 0.49 mol% --- and peptide bonds without an arrangement of Arg-Gly-Asp (RGD) as a cell-adhesion molecule, or probably the existence of a

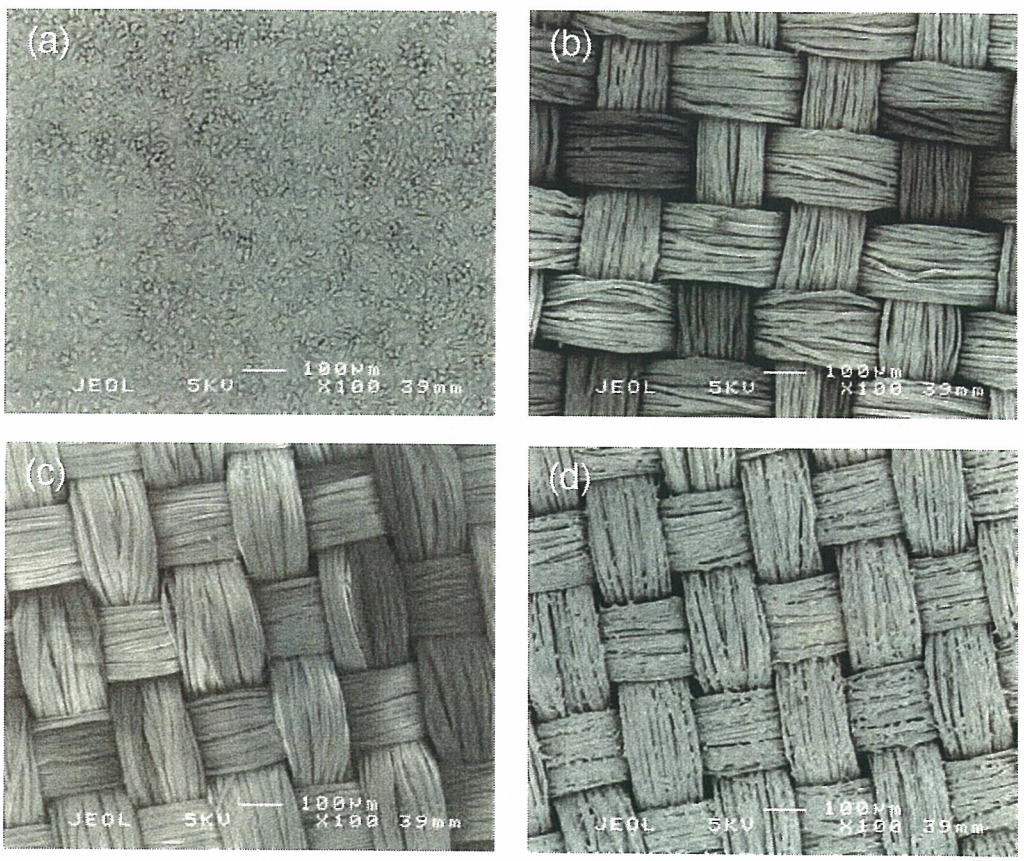

Fig. 3 SEM photographs of cell morphologies on (a) gelatin-coated grass, (b) original SF fabric, (c) hydrolysed poly(MPTS)-frafted SF fabric, and (d) calcined HAp nanopartilces covalently coated on an SF fabric.

microdomain structure consisting of crystalline and amorphous regions attributed to an arrangement of $(Gly\text{-}Ala\text{-}Ser)_n$ and the other residues in SF . The cells indicated weak interaction with the hydrolyzed poly(MPTS)-grafted surface during the initial incubation period because of the surface hydrophilicity belonging to Si-OH moieties on Si-O-Si cross-linking networks produced by hydrolysis of the poly(MPTS)-grafted SF substrate. Meanwhile, the cells adhered well on HAp-coated SF as shown in **Fig. 3 (d)**. It is clear that cells, thus, favorably adhere only on the HAp surface of the composite but not on the dehydrated grafted-surface without HAp particles on the SF substrate. It is estimated that cell-adhesion proteins in serum, such as fibronectin, vitronectin, bFGF, etc., prior to cell adhesion, adsorb on a HAp surface much better than on an area of dehydrated graft-polymer. That is to say, the surface of the HAp nanocoating can provide bioactivity to a polymer substrate.

Fabrication of Medical Devices

A Percutaneous Device. To fabricate a prototype for a percutaneous device, the HAp-coated SF fibers were transplanted onto a button-shaped substrate made of silicone via an adhesive agent. The percutaneous device was implanted in back of a rabbit for 3 months according to the Guideline for Animal Experimentation National Cardiovascular Center. The skin tissue was adhered on the device without a gap between the tissue and the material surface, and severe inflammation and abscess was not observed from the external view (**Fig. 4**).

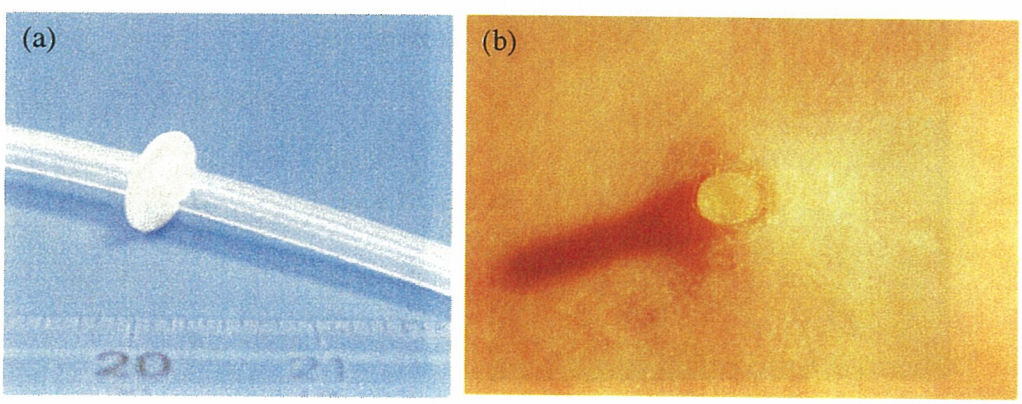

Fig. 4 External views of the button prototype of a percutaneous device (a) and the surrundings of the device implanted into back of a rabbit for 3 months.

An Artificial Blood Vessel. We developed a novel inorganic-organic composite consisting of calcined HAp nanoparticles chemically bonded on polymer substrate. HAp nanoparticles were covalently linked onto a poly(ethylene terephthalate) (PET) fabric substrate chemically modified by graft polymerization with MPTS for development of artificial blood vessel. A prototype of artificial blood vessel made of the HAp/PET composite was fabricated (**Fig. 5**). The calcined HAp nanoparticles were thoroughly coated on PET fibers of inside and outside of an artificial blood vessel [9]. The effect of HAp nanocrystals on it through animal implantation experiments *in vivo* are evaluating now.

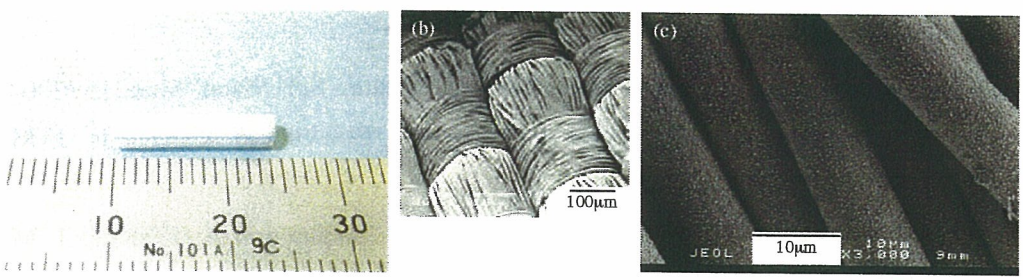

Fig. 5 Images show prototype of an artificial blood vessel made of HAp/PET composite. (a) External view of the prototype. (b, c) lower and higher magnification of SEM images of HAp/PET fibers of inside of the prototype.

Conclusions

The inorganic-organic composite consisting of calcined HAp nanoparticles and polymer substrates were prepared through chemical bonding, such as covalent or ionic bonding. Preparation of composites consisting of calcined HAp nanoparticles and polymer substrates, for examples, mixture, *in situ* or nano-chemical bonding methods, is necessary for nano-scaled observation from the points of view of the bulk structures, surface properties, biological interactions, etc. For our composite, especially, the size, coverage ratio or strength of chemical bonding of sintered HAp nanoparticles assumed to be very important to know interactions with biomolecules such as proteins, cells, tissues to develop medical devices. This composite material is expected to establish a novel concept for fabrication of an inorganic-organic composite

as biocompatible materials for hard and soft tissue.

Acknowledgements

The authors are grateful to Dr. M. Okada and Mr. S. Yasuda, National Cardiovasucular Center research Institute, for their supports. The study was financially supported in part of Innovation Plaza Osaka, Japan Science and Technology Corporation (JST) and promoting projects on Comprehensive Research on Cardiovascular Diseases.

References

[1] T. Furuzono, D. Walsh, K. Sato, K. Sonoda and J. Tanaka: J. Mater. Sci. Lett. 20 (2001), 111.

[2] T. Furuzono, A. Kishida and J. Tanaka: J. Mater. Sci. Mater. Med. 15 (2004), 19.

[3] A. Korematsu, T. Furuzono, S. Yasuda, J. Tanaka and A. Kishida: J. Mater. Sci. 39,(2004), 3221.

[4] A. Korematsu, T. Furuzono, S. Yasuda, J. Tanaka and A. Kishida: J. Mater. Sci. Mater. Med. 16 (2005), 6.

[5] T. Furuzono, S. Yasuda, T. Kimura, Si. Kyotani, J. Tanaka and A. Kishida: J. Artif Organis 7 (2004), 137.

[6] M. Okada and T. Furuzono: J. Nanosci. Nanotech, in press.

[7] M. Okada and T. Furuzono: J. Mater. Sci. Lett. in contribution.

[8] M. Okada and T. Furuzono: J. Nanoparticle Res. in contribution.

[9] T. Furuzno, M. Masuda, M. Okada, S. Yasuda, H. Kadono, R. Tanaka and K. Miyatake: ASAIO J. in press.

J Mater Sci (2006) 41:6134–6137
DOI 10.1007/s10853-006-0444-6

LETTER

Fabrication of high-dispersibility nanocrystals of calcined hydroxyapatite

Masahiro Okada · Tsutomu Furuzono

Received: 7 October 2005 / Accepted: 10 May 2006 / Published online: 12 August 2006

Hydroxyapatite (HAp) is a major inorganic component of bone and teeth. Artificially synthesized HAp has been extensively used in a variety of applications, such as biomaterials, ion exchangers, adsorbents, and catalysts, by exploiting its biocompatibility and adsorbability of many compounds. When low-crystallinity HAp nanoparticles are calcined to increase thermal and chemical stability, the particles typically sinter into a large agglomerate consisting of polycrystal [1–5]. Thus, calcined HAp crystals dispersed in liquid medium on a nanoscale have been difficult to obtain. This paper describes the fabrication of HAp nanocrystals by calcination with an anti-sintering agent interspersed between the particles and the subsequent removal of the agent. The HAp nanocrystals obtained here should be suitable for the above applications owing to their high dispersibility in liquid media, high specific surface area, and high thermal and chemical stability.

We have recently developed a novel inorganic/organic composite for a soft-tissue-compatible material: a flexible silicone elastomer [6] or a silk fibroin [7], whose surface was modified with calcined HAp crystals. After the HAp crystals dispersed in a liquid medium were adsorbed on the substrate, chemical reaction at their interface between the HAp crystals and the substrate was conducted to connect them through covalent bonding. The novel composite retained flexibility of the polymer substrate and showed improved tissue adhesion with the HAp crystals on the surface [8]. Throughout these studies, the HAp crystals were used after calcination at 800 °C to reduce in vivo absorbability. As mentioned above, HAp nanoparticles mostly sinter into large agglomerates of polycrystals during calcination. This made it difficult to control the surface morphology of the composite because the agglomerates had poor dispersibility in liquid media and large size distribution.

Hydrothermal treatment of HAp particles in water medium under high pressure is known to enable the preparation of agglomerate-free HAp crystals [9–11]. However, this treatment generally leads to an increase in crystal size due to Ostwald ripening [12, 13], and is restricted to laboratory-scale products as it is a high-pressure process.

The present study reports the fabrication of nanosized and calcined HAp crystals protected against calcination-induced sintering using an anti-sintering agent interspersed between the particles. Thus, there was no contact between the crystals during calcination. Calcium hydroxide [$Ca(OH)_2$] was selected as an anti-sintering agent because it would not melt at the calcination temperature (800 °C), presumably not dissolve HAp, and could be removed by washing with water after calcination.

Starting HAp particles with low crystallinity were prepared with a modified emulsion system at 25 °C [14]. The resulting product was centrifugally washed and redispersed in water (solid content: 5 wt%). In order to intersperse $Ca(OH)_2$ between the particles, the HAp aqueous dispersion was added into a saturated aqueous $Ca(OH)_2$ solution (0.17 wt%), and the mixture was dried under reduced pressure at 40 °C. The resultant

M. Okada · T. Furuzono (✉)
Department of Bioengineering, Advanced Medical Engineering Center, National Cardiovascular Center Research Institute, 5-7-1 Fujishirodai, Suita, Osaka 565-8565, Japan
e-mail: furuzono@ri.ncvc.go.jp

HAp/$Ca(OH)_2$ (1/1, w/w) mixture was calcined at 800 °C for 1 h in air (heating rate: 10 °C/min). After calcination, the mixture was centrifugally washed with water to remove the $Ca(OH)_2$. As a control procedure, the same starting HAp particles were calcined without adding $Ca(OH)_2$.

First, in order to examine the effect of $Ca(OH)_2$ on the crystal phase and composition of HAp, X-ray diffraction (XRD; RAD-X, Rigaku International Co., Tokyo, Japan) with CuKα radiation and Fourier-transform infrared (FTIR) spectroscopy (Spectrum One, Perkin-Elmer Inc., MA, USA) were performed as shown in Fig. 1. In Fig. 1a and b, both XRD profiles showed highly crystalline HAp, and no other calcium phosphate phases could be detected. In the FTIR spectrum of HAp calcined with $Ca(OH)_2$ shown in Fig. 1d, a peak at 3,640 cm^{-1} due to stretching of OH in $Ca(OH)_2$ was not observed, indicating complete removal of $Ca(OH)_2$. Bands at 877 and 1,413/1,456 cm^{-1} observed in both the FT-IR spectra are attributed to CO_3^{2-} substituting phosphate positions in HAp lattice [15], and came from atmospheric carbon dioxide under high solution pH during the preparation of the starting HAp. A new peak at 3,544 cm^{-1} in Fig. 1d seems to be due to the formation of calcium-rich apatite (Ca/P atomic ratio > 1.67) [16]. It is worth pointing out that the Ca/P atomic ratio of the HAp calcined with $Ca(OH)_2$ (Ca/P = 1.58) slightly increased as compared with that without additives (Ca/P = 1.56) measured by inductively coupled plasma-atomic emission spectrometry (SPS4000, Seiko Instrument Inc., Chiba, Japan). These results might suggest the formation of calcium-rich apatite from the crystal surface during calcination, by migration of calcium ions from $Ca(OH)_2$ on the calcium-deficient crystal.

The HAp crystals were observed by scanning electron microscopy (JSM-6301F, JEOL Ltd., Tokyo, Japan) and transmission electron microscopy (JEM-2000 EXII, JEOL Ltd.) as shown in Fig. 2. Single-crystal size (or grain size of polycrystal) was measured from the micrographs, and is presented as "mean ± SD" (N = 100). The crystal sizes were not statistically different between the HAp crystals calcined without and with $Ca(OH)_2$ (52.5 ± 15.4 nm for calcination without additives; 55.7 ± 15.1 nm for calcination with $Ca(OH)_2$). Although some agglomerates were observed in Fig. 2b, it is difficult to judge whether the agglomerates were polycrystals or not. This is because the micrograph was taken under dry condition and nano-sized particles generally tend to gather due to a capillary force of the medium between the particles during the drying of the medium.

Therefore, the dispersibility of the HAp crystals was evaluated form the dispersed-particle size, which was measured in ethanol medium by dynamic light scattering (DLS; ELS-8000, Otsuka Electronics Co., Ltd., Kyoto, Japan) at 10-ppm concentration and a light-scattering angle of 90° (Fig. 3). In the case of calcination without

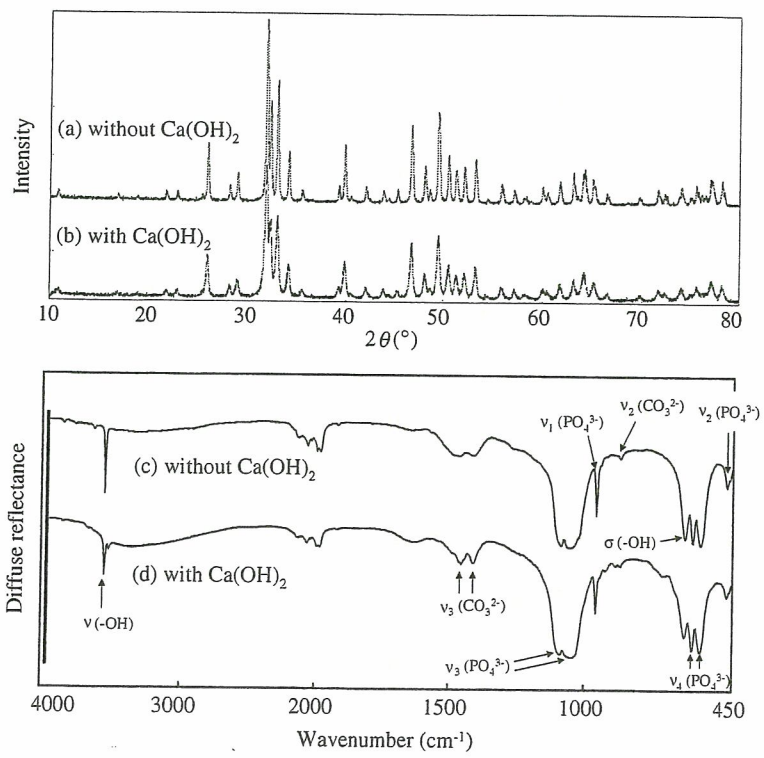

Fig. 1 X-ray diffraction patterns (**a**, **b**) and FTIR spectra (**c**, **d**) of hydroxyapatite (HAp) particles calcined at 800 °C for 1 h without (**a**, **c**) and with (**b**, **d**) $Ca(OH)_2$ (HAp/$Ca(OH)_2$ = 1/1 w/w) interspersed between the particles. $Ca(OH)_2$ was centrifugally washed off with an aqueous solution after calcination

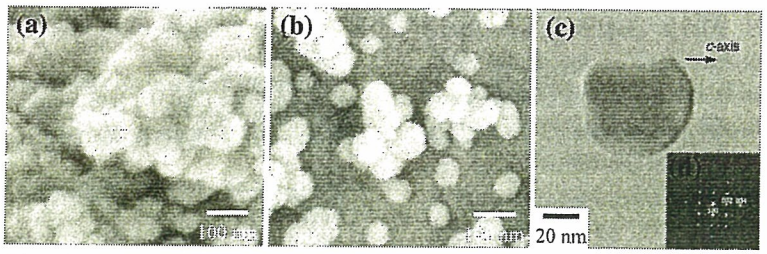

Fig. 2 SEM photographs (**a**, **b**) of HAp crystals calcined without (**a**) and with (**b**) $Ca(OH)_2$. A TEM photograph (**c**) and the associated electron diffraction pattern corresponding to the [210] zone (**d**) of a HAp crystal calcined with $Ca(OH)_2$, showing that the crystal consisted of a single HAp phase

additives, the dispersed-particle size (664.0 ± 382.0 nm) was much larger than the crystal size (52.5 ± 15.4 nm), which indicates the formation of polycrystals of sintered HAp. On the other hand, the dispersed-particle size of the HAp calcined with $Ca(OH)_2$ was 126.3 ± 79.0 nm. This indicates that sintering between the HAp nanocrystals can be mostly prevented by interspersing $Ca(OH)_2$ between the crystals prior to calcination.

However, the dispersed-particles size (126.3 ± 79.0 nm) was larger than the crystal size (55.7 ± 15.1 nm) measured by electron microscope. This suggest that some particles contacted with each other before the deposition of $Ca(OH)_2$ from the aqueous solution. In order to avoid the contact, poly(acrylic acid) (PAA) was used. PAA can act as a dispersion stabilizer by adsorbing on HAp surfaces [17, 18], and an addition of calcium ions into an aqueous PAA solution induces a rapid precipitation of poly(acrylic acid calcium salt) (PAA-Ca). Therefore, it is expected that PAA-Ca precipitates onto the separated HAp particle by addition of calcium ions into the PAA-adsorbed HAp particles. Although the organic component of PAA-Ca will be decomposed during calcination at 800 °C, the thermally decomposed product (CaO) remains on the crystals and presumably acts as an anti-sintering agent.

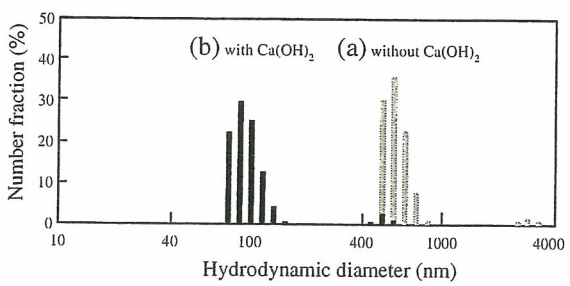

Fig. 3 The dispersed-particle sizes of HAp crystals calcined without (**a**) and with (**b**) $Ca(OH)_2$, measured in ethanol medium

In the present study, PAA (Sigma-Aldrich Co.; weight-average molecular weight = 15,000; HAp/PAA = 1/1 w/w) was added at pH 10, and $Ca(OH)_2$-saturated aqueous solution ($Ca(OH)_2$/COOH in PAA = 1/1 molar ratio) was added to precipitate PAA-Ca. The resultant HAp/PAA-Ca mixture was calcined in the same manner described above, and then washed with water to remove CaO.

The resultant HAp crystals are shown in Fig. 4. The dispersed-particle size of the HAp crystals in ethanol (45.0 ± 14.9 nm) was not statistically different from the crystal size (53.4 ± 16.2 nm) measure by electron microscope. This result indicates that HAp nanocrystals calcined with PAA-Ca can be dispersed as single crystals. IR spectrum and XRD pattern of the HAp single crystals calcined with PAA-Ca were almost the same as those shown in Fig. 1b and d, and Ca/P atomic ratio was 1.58. The achieved high dispersibility of HAp single crystals should be due to the absence of the calcination-induced sintering and might be due to cationic charge of the calcium-rich surface.

Fig. 4 A SEM photograph (**a**) and the dispersed-particles size (**b**) of HAp crystals calcined at 800 °C for 1 h with poly(acrylic acid calcium salt) (PAA-Ca) surrounding the particles. CaO, the thermally decomposed product of PAA-Ca, was centrifugally washed off with an aqueous solution after calcination

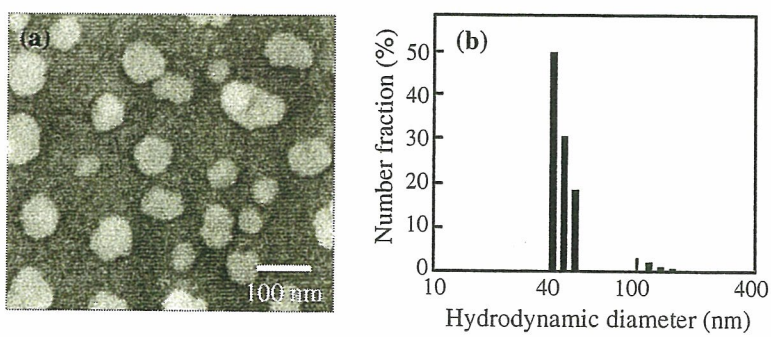

In summary, calcined HAp nanocrystals were successfully fabricated by calcination using an anti-sintering agent interspersed between or surrounding the particles, followed by removal of the agent. The HAp nanocrystals obtained here should be suitable for the various applications mentioned above, and also as dental and orthopedic ultrafine fillers for microporosity owing to their high dispersibility in liquid media and high thermal and chemical stability. Calcination with an anti-sintering agent has a potential application to a wide range of calcined nanoceramic powders, such as alumina, titania, and magnesia, and offer significant benefits over existing technologies because the technique is simple, inexpensive, and amenable to scale-up and processing.

Acknowledgments We thank Dr. K. Sato of the Advanced Manufacturing Research Institute, National Institute of Advanced Industrial Science and Technology (AIST), for helpful discussions. This work was partially supported by a grant from PRESTO, Japan Science and Technology Agency, and a Research Grant for Cardiovascular Diseases from the Ministry of Health, Labour and Welfare, Japan.

References

1. Frenkel J (1945) J Phys USSR 9:385
2. Kuczynski GC (1949) Trans AIME 185:169
3. Barralet JE, Best SM, Bonfield W (2000) J Mat Sci Mater Med 11:719
4. Landi E, Tampieri A, Celotti G, Sprio S (2000) J Eur Ceram Soc 20:2377
5. Bernache-Assollant D, Ababoua A, Championa E, Heughebaertb M (2003) J Eur Ceram Soc 23:229
6. Furuzono T, Sonoda K, Tanaka J (2001) J Biomed Mater Res 56:9
7. Furuzono T, Kishida A, Tanaka J (2004) J Mater Sci Mater Med 15:19
8. Furuzono T, Wang P, Korematsu A, Miyazaki K, Oido-Mori M, Kowashi Y, Ohura K, Tanaka J, Kishida A (2003) J Biomed Mater Res B Appl Biomater 65B:217
9. Somiya S, Ioku K, Yoshimura M (1988) Mater Sci Forum 34–36:371
10. Yoshimura M, Suda H, Okamoto K, Ioku K (1994) J Mater Sci 29:3399
11. Papargyris AD, Botis AI, Papargyri SA (2002) Key Eng Mater 206–213:83
12. Carless JE, Foster AA (1966) J Pharm Pharmacol 18:697
13. Wei M, Ruys AJ, Milthorpe BK, Sorrell CC (1999) J Biomed Mater Res 45:11
14. Furuzono T, Walsh D, Sato K, Sonoda K, Tanaka J (2001) J Mater Sci Lett 20:111
15. Emerson WH, Fisher EE (1962) Arch Biol 7:671
16. Bonel G, Heughebaert J-C, Heughebaert M, Lacout JL, Lebugle A (1988) Ann NY Acad Sci 523:115
17. Misra DN (1993) J Dent Res 10:1418
18. Yoshida Y, Van Meerbeek B, Nakayama Y, Yoshioka M, Snauwaert J, Abe Y, Lambrechts P, Vanherle G, Okazaki M (2001) J Dent Res 80:1565

Journal of
Nanoscience and Nanotechnology
Vol. 7, 1–4, 2007

Nano-Sized Ceramic Particles of Hydroxyapatite Calcined with an Anti-Sintering Agent

Masahiro Okada and Tsutomu Furuzono*

Department of Bioengineering, Advanced Medical Engineering Center,
National Cardiovascular Center Research Institute, 5-7-1 Fujishirodai, Suita, Osaka 565-8565, Japan

Nano-sized crystals of calcined hydroxyapatite (HAp) having spherical morphologies were fabricated by calcination at 800 °C for 1 h with an anti-sintering agent surrounding the original HAp particles and the agent was subsequently removed by washing after calcination. The original HAp particles were prepared by a modified emulsion system, and surrounded with poly(acrylic acid, calcium salt) (PAA-Ca) by utilizing a precipitation reaction between calcium hydroxide and poly(acrylic acid) adsorbed on the HAp particle surfaces in an aqueous medium. In the case of calcination without PAA-Ca, micron-sized particles consisting of sintered polycrystals were mainly observed by scanning electron microscopy, indicating the calcination-induced sintering among the crystals. On the other hand, most of the crystals calcined with the anti-sintering agent were observed as isolated particles, and the mean size of the HAp crystals was around 80 nm. This result indicates that PAA-Ca and its thermally decomposed product, CaO, surrounding the HAp crystals could protect them against calcination-induced sintering during calcination at 800 °C. The HAp crystals calcined with PAA-Ca showed high crystallinity, and no other calcium phosphate phases could be detected.

Keywords:

RESEARCH ARTICLE

1. INTRODUCTION

Hydroxyapatite (HAp, $Ca_{10}(PO_4)_6(OH)_2$) ceramic is an important biomaterial and has been widely used by taking into account its biocompatibility, because its constituent is chemically similar to those of the mineral of bones and teeth. HAp also has been extensively used in a variety of applications, such as adsorbents, carrier for drug delivery system, ion exchangers, and catalysts, by exploiting its adsorbability of many compounds and biocompatibility. However, owing to its mechanical weakness and brittleness,[1–3] applications of HAp have been confined to those with low mechanical stress. We recently developed a novel inorganic/organic composite:[4,5] a flexible polymer substrate, whose surface was modified with calcined HAp nanoparticles through covalent bonding. The novel composite retained the flexibility of the polymer substrate and showed surface properties of HAp such as tissue adhesion in a living body.

Throughout these studies, the HAp particles were prepared by a modified emulsion system[6,7] and used after calcination at 800 °C to reduce sorbability *in vivo*. When low-crystallinity HAp nanoparticles are calcined to increase thermal and chemical stability, the particles sinter randomly into large agglomerates consisting of polycrystals.[8–12] Therefore, calcined HAp crystals on a nanoscale have been difficult to obtain. Because the sintered polycrystals has poor dispersibility in liquid media and a large size distribution, it was difficult to control the surface morphology (covering ratio, surface roughness) of the above-mentioned composite. Hydrothermal treatment of HAp particles in an aqueous medium under high pressure is known to enable the preparation of agglomerate-free HAp crystals.[13–15] However, this treatment generally leads to an increase in crystal size due to Ostwald ripening,[16,17] and is restricted to laboratory-scale products as it is a high-pressure process.

In this article, nano-sized and calcined HAp crystals protected against calcination-induced sintering will be fabricated by using an anti-sintering agent surrounding the HAp particles. Thus, there was no contact between the particles during calcination. Calcium hydroxide [$Ca(OH)_2$] was selected as a component of the anti-sintering agent because it would not melt at the calcination temperature (800 °C), presumably not dissolve the HAp, and could be removed by washing with water after calcination. In order to surrounding the HAp particles efficiently with the anti-sintering agent, a precipitation reaction between $Ca(OH)_2$ and poly(acrylic acid) (PAA) adsorbed on the HAp particles in an aqueous medium was utilized. The obtained

*Author to whom correspondence should be addressed.

1533-4880/2007/7/001/004 doi:10.1166/jnn.2007.505

crystals were evaluated by means of X-ray diffraction (XRD) measurement, Fourier-transform infrared (FT-IR) spectroscopy, and scanning electron microscope (SEM) observation.

2. EXPERIMENTAL DETAILS

2.1. Materials

$Ca(OH)_2$ was prepared by the hydrolysis of calcium oxide, which was obtained by calcination of alkaline-analysis-grade calcium carbonate ($CaCO_3$; Wako Pure Chemical Industries, Ltd., Osaka, Japan) at 1050 °C for 3 h. PAA (weight-average molecular weight: 15,000) used as a polymeric stabilizer was purchased from Sigma-Aldrich Co., MO, USA. Other materials were reagent grade and purchased from Nacalai Tesque Inc., Kyoto, Japan. Milli-Q water with a specific resistance of 18.2×10^6 Ω · cm was used (Millipore Corp., MA, USA).

2.2. Calcination of HAp Particles

Starting HAp particles with low crystallinity were prepared by a modified emulsion system at 25 °C using $Ca(OH)_2$ and potassium dihydrogen phosphate, according to the previous articles.[6,7] The particles prepared was centrifugally washed with water and redispersed in water (solid content: 5 wt%). The calcination procedure of HAp particles with the anti-sintering agent is sketched in Figure 1. An amount of PAA, approximately equal in weight to the HAp particles, was dissolved in water at 1.0 wt%, and the pH of the PAA *aq.* was adjusted to 10.0. The PAA *aq.* was added in the HAp dispersion, and the dispersion was ultrasonicated for 5 min. An excess amount of calcium ions was added to the dispersion in the form of a saturated $Ca(OH)_2$ *aq.* ($Ca(OH)_2$/COOH in PAA = 1/1 molar ratio) to precipitate poly(acrylic acid, calcium salt) (PAA-Ca) onto the HAp particles. The resultant HAp/PAA-Ca mixture was filtered, dried at 80 °C for 2 h under reduced pressure, and calcined at 800 °C for 1 h at a heating rate of 10 °C/min. Calcination was carried out in a horizontal furnace with an alumina tube in air. In order to remove the thermal decomposed product of PAA-Ca, CaO, after calcination, the mixture was centrifugally washed with 100 mM NH_4NO_3 *aq.* under N_2 to reduce the formation of $CaCO_3$ by the reaction between calcium ion and carbon dioxide in air, until the pH of the aqueous dispersion decreased to almost 7.0, and then washed further with water three times. To investigate the effect of the anti-sintering agent, the HAp particles were calcined with the same procedure, but without adding PAA and $Ca(OH)_2$.

2.3. Measurements

Identification of the product was conducted by XRD measurement (RAD-X; Rigaku International Co., Tokyo, Japan) with CuK_α radiation, and diffuse reflectance FT-IR spectroscopy (Spectrum One; Perkin-Elmer Inc., MA, USA). The size and morphology of the HAp crystals were observed by SEM (JSM-6301F; JEOL Ltd., Tokyo, Japan). The Ca/P atomic ratio of each HAp was measured by inductively coupled plasma-atomic emission spectrometry (ICP-AES: SPS4000; Seiko Instrument Inc., Chiba, Japan). Calcium and phosphorus standard solutions for ICP-AES were purchased from Kanto Chemical Co., Inc., Tokyo, Japan.

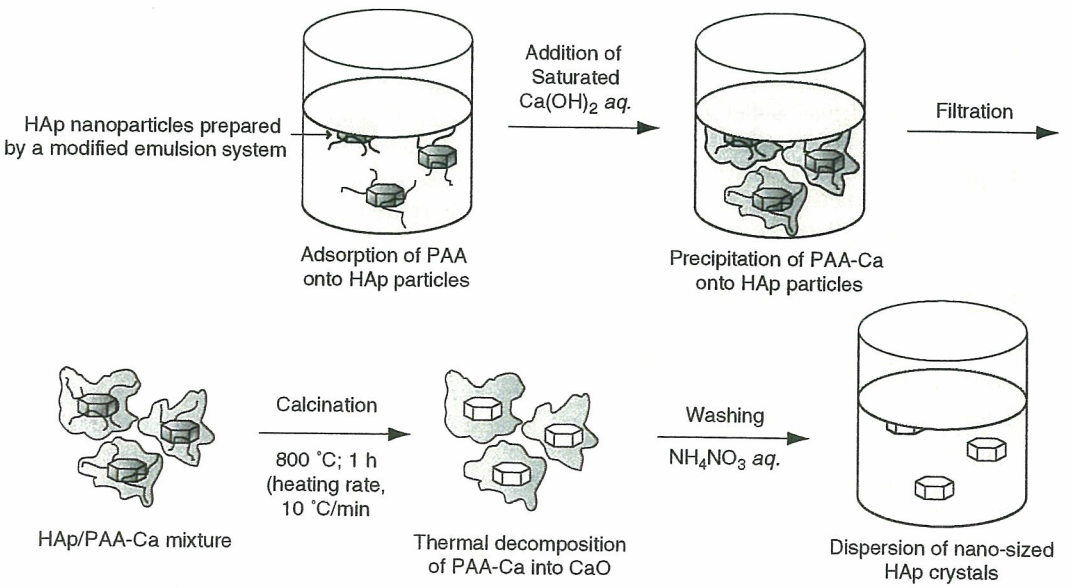

Fig. 1. A schematic model for the fabrication of nano-sized crystals of hydroxyapatite by calcination with an anti-sintering agent surrounding the crystals and subsequent removal of the agent.

RESEARCH ARTICLE

3. RESULTS AND DISCUSSION

In order to surround the particles with the anti-sintering agent, PAA was adsorbed on the surfaces of the HAp particles in an aqueous medium. PAA can adsorb on HAp surfaces,[18–19] and thus act as a polymeric dispersant to prevent flocculation of HAp particles in an aqueous medium. An addition of calcium ions into an aqueous PAA solution under alkaline condition induces precipitation of PAA-Ca. Accordingly, when $Ca(OH)_2$ *aq.* is added to the PAA-stabilized HAp dispersion, PAA-Ca would precipitate onto the surfaces of the HAp particles. The PAA-Ca presumably acts as an anti-sintering agent, because there is no contact among the HAp particles by surrounding them with PAA-Ca and its thermally decomposed product, CaO, during calcination.

First, the influence of PAA-Ca on the crystal phase and composition of HAp were investigated. Figure 2(a) shows the XRD profile of the HAp particles after calcination with PAA-Ca. From the profile, highly crystallized HAp was detected, and no other calcium phosphate phases such as tricalcium phosphate could be detected. The Ca/P ratio of the HAp calcined with PAA-Ca was 1.58 (1.56 in the case of the HAp calcined without additives), indicating the formation of calcium-deficient HAp with high crystallinity after calcination with PAA-Ca.

In the FT-IR spectrum shown in Figure 2(b), the absorption bands at 603/572 and 474 cm^{-1} are respectively attributed to $\nu_4PO_4^{3-}$ and $\nu_2PO_4^{3-}$ in crystalline HAp. Absorptions at 1092/1045 and 963 cm^{-1} are respectively attributed to $\nu_3PO_4^{3-}$ and $\nu_1PO_4^{3-}$. The sharp absorptions of OH stretching and deformation vibrations at 3573 and 632 cm^{-1} indicate that the material exhibits high crystallinity after calcination. Bands at 1456/1413 and 877 cm^{-1}, attributed to CO_3^{2-} substituting phosphate positions in the HAp lattice.[20] The carbonate ion should be from atmospheric carbon dioxide during the preparation of the original HAp particles and from carbon dioxide generated by thermal decomposition of PAA-Ca during calcination.

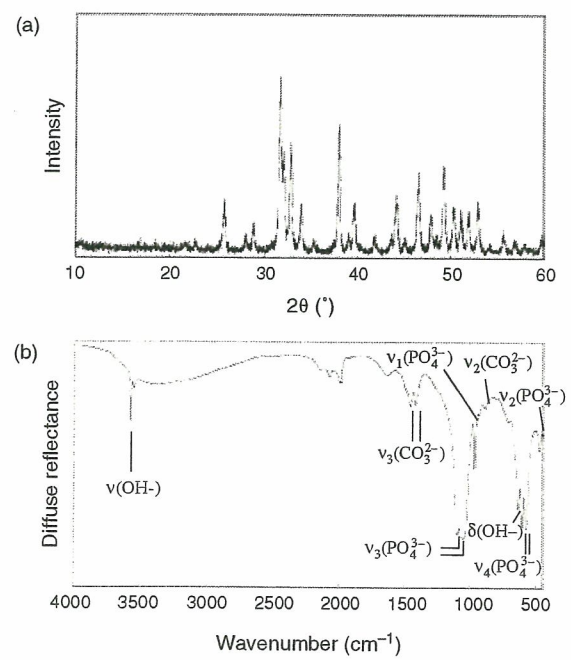

Fig. 2. X-ray diffraction pattern (a) and FT-IR spectrum (b) of HAp crystals calcined at 800 °C for 1 h with PAA-Ca surrounding the particles. The thermal decomposed product of PAA-Ca, CaO, was centrifugally washed with an aqueous solution after calcination.

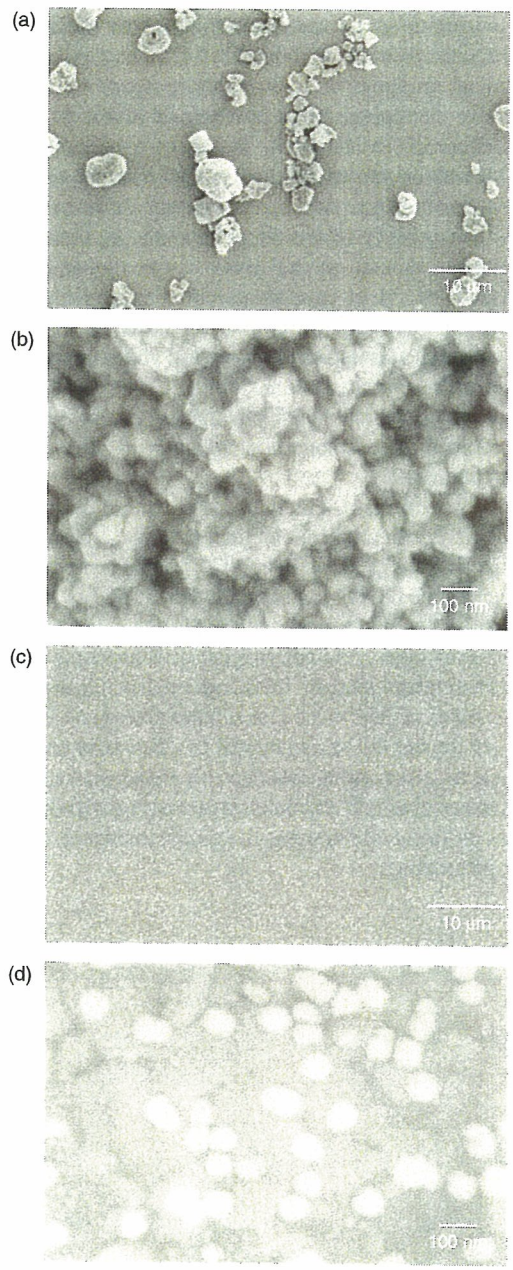

Fig. 3. Lower magnified (a, c) and higher magnified (b, d) SEM photographs of HAp crystals calcined without additives (a, b) and with PAA-Ca (c, d).

RESEARCH ARTICLE

It should be noted that peak at 3644 cm^{-1} due to the stretching of OH in $Ca(OH)_2$ and the peaks at 1453/1415 cm^{-1} corresponding to the CH_2 and CH bending mode of the PAA chain were not found, suggesting complete removal of the anti-sintering agent by the thermal decomposition and the centrifugal washing with water. A small peak at 3544 cm^{-1}, which was not observed in the case of calcination without additives, was additionally observed after calcination with PAA-Ca. The origin of the additional peak is under investigation, and will be reported in the near future.

Figure 3 shows the morphologies of the HAp crystals calcined with or without PAA-Ca. Crystals with spherical or irregular morphologies were observed, irrespective of the presence or absence of PAA-Ca as shown in Figures 3(b) and (d). In the case of calcination without additives shown in Figure 3(a) with lower magnification, micron-sized particles consisting of sintered polycrystals were mainly observed, indicating the calcination-induced sintering among the crystals. On the other hand, in the case of the HAp crystals calcined with the anti-sintering agent shown in Figure 3(c), most of the crystals were observed as isolated particles, and the mean size of the particles was around 80 nm. This indicates that sintering among the HAp nanocrystals could be mostly prevented by surrounding them with PAA-Ca prior to calcination.

In summary, calcined HAp nanocrystals were successfully fabricated by calcination with an anti-sintering agent surrounding the particles, followed by removal of the agent. The HAp nanocrystals fabricated here should be suitable for the various applications such as biomaterials, ion exchangers, adsorbents, and catalysts owing to their high dispersibility in liquid media and high thermal and chemical stability. The calcination with an anti-sintering agent should be applicable to other nanoceramic powders, such as alumina, titania, and magnesia, and have significant benefits over existing technologies, because the methods is facile, inexpensive, and amenable to scale-up and processing.

Acknowledgments: We thank Dr. K. Sato of the Advanced Manufacturing Research Institute, National Institute of Advanced Industrial Science and Technology (AIST), for helpful discussions. This work was supported by a Research Grant for Cardiovascular Diseases from the Ministry of Health, Labour, and Welfare, Japan.

References and Notes

1. H. Aoki, Science and Medical Application of Hydroxyapatite, Takayama Press System Center Co., Inc. (**1991**).
2. W. Suchanek, M. Yashima, M. Kakihana, and M. Yoshimura, *J. Am. Ceram. Soc.* 80, 2805 (**1997**).
3. C. R. Kothaplli, M. Wei, R. Z. Legeros, and M. T. Shaw, *J. Mater. Sci.: Mater. Med.* 16, 441 (**2005**).
4. T. Furuzono, K. Sonoda, and J. Tanaka, *J. Biomed. Mater. Res.* 56, 9 (**2001**).
5. T. Furuzono, S, Yasuda, T. Kimura, S. Kyotani, J. Tanaka, and A. Kishida, *J. Artif. Organs* 7, 137 (**2004**).
6. T. Furuzono, D. Walsh, K. Sato, K. Sonoda, and J. Tanaka, *J. Mater. Sci. Lett.* 20, 111 (**2001**).
7. K. Sonoda, T. Furuzono, D. Walsh, K. Sato, and J. Tanaka, *Solid State Ionics* 151, 321 (**2002**).
8. J. Frenkel, *J. Phys. USSR* 9, 385 (**1945**).
9. G. C. Kuczynski, *Trans. AIME* 185, 169 (**1949**).
10. J. E. Barralet, S. M. Best, and W. Bonfield, *J. Mater. Sci.: Mater. Med.* 11, 719 (**2000**).
11. E. Landi, A. Tampieri, G. Celotti, and S. Sprio, *J. Eur. Ceram. Soc.* 20, 2377 (**2000**).
12. D. Bernache-Assollant, A. Ababoua, E. Championa, and M. Heughebaertb, *J. Eur. Ceram. Soc.* 23, 229 (**2003**).
13. S. Somiya, K. Ioku, and M. Yoshimura, *Mater. Sci. Forum* 34–36, 371 (**1988**).
14. M. Yoshimura, H. Suda, K. Okamoto, and K. Ioku, *J. Mater. Sci.* 29, 3399 (**1994**).
15. A. D. Papargyris, A. I. Botis, and S. A. Papargyri, *Key Eng. Mater.* 206–213, 83 (**2002**).
16. J. E. Carless and A. A. Foster, *J. Pharmaceut. Pharmacol.* 18, 697 (**1966**).
17. M. Wei, A. J. Ruys, B. K. Milthorpe, and C. C. Sorrell, *J. Biomed. Mater. Res.* 45, 11 (**1999**).
18. D. N. Misra, *J. Dent. Res.* 10, 1418 (**1993**).
19. Y. Yoshida, B. Van Meerbeek, Y. Nakayama, M. Yoshioka, J. Snauwaert, Y. Abe, P. Lambrechts, G. Vanherle, and M. Okazaki, *J. Dent. Res.* 80, 1565 (**2001**).
20. W. H. Emerson and E. E. Fisher, *Arch. Oral. Biol.* 7, 671 (**1962**).

Received: 6 November 2005. Accepted: 13 March 2006.

RESEARCH ARTICLE

Journal of Nanoparticle Research (2006)
DOI 10.1007/s11051-006-9126-1

Calcination of rod-like hydroxyapatite nanocrystals with an anti-sintering agent surrounding the crystals

M. Okada and T. Furuzono*
*Department of Bioengineering, Advanced Medical Engineering Center, National Cardiovascular Center Research Institute, 5-7-1 Fujishirodai, Suita, Osaka, 565-8565, Japan; *Author for correspondence (E-mail: furuzono@ri.ncvc.go.jp)*

Received 10 October 2005; accepted in revised form 4 May 2006

Key words: hydroxyapatite, nanocrystal, calcination, dispersion, thermal decomposition, sintering

Abstract

Sintering-free nanocrystals of calcined hydroxyapatite (HAp) having a rod-like morphology were fabricated by calcination at 800°C for 1 h with an anti-sintering agent surrounding original HAp particles and the agent was subsequently removed after calcination. The original HAp particles having a rod-like morphology with a size ranging from 30 to 80 nm (short axis) and 300 to 500 nm (long axis) were prepared by wet chemical process, and poly(acrylic acid, calcium salt) (PAA-Ca) was used as the anti-sintering agent. In the case of calcination without additives, the mean size of HAp crystals dispersed in an ethanol medium increased by about 4 times and the specific surface area of the crystals exhibited a 25% decrease compared to those of the original HAp particles because of calcination-induced sintering among the crystals. On the other hand, the HAp crystals calcined with the anti-sintering agent, PAA-Ca, could be dispersed in an ethanol medium at the same size as the original particles, and they preserved the specific surface area after calcination. These results indicate that PAA-Ca and/or its thermally decomposed product, CaO, surrounded the HAp particles and protected them against calcination-induced sintering during calcination. The HAp crystals calcined with PAA-Ca showed high crystallinity, and no other calcium phosphate phases could be detected after washing with water.

Introduction

Hydroxyapatite (HAp, $Ca_{10}(PO_4)_6(OH)_2$) is ideal as the main mineral of bones and teeth. Artificially synthesized HAp has been extensively used in a variety of applications, such as biomaterials, ion exchangers, adsorbents, and catalysts by exploiting its biocompatibility and adsorbability with many compounds. However, owing to its mechanical weakness and brittleness (Aoki, 1991; Suchanek et al., 1997), applications of HAp have been confined to those with low mechanical stress. In order to overcome the weakness of HAp, we have recently developed a novel inorganic/organic composite as a soft-tissue compatible material: a flexible silicone elastomer (Furuzono et al., 2001) or a silk fibroin (Furuzono et al., 2004), whose surface was modified with calcined HAp crystals through covalent bonding. The novel composite retained the flexibility of the polymer substrate and showed good tissue adhesion due to the HAp crystals on the surface (Furuzono et al., 2003). Throughout these studies, the HAp crystals were used after calcination at 800°C to reduce *in vivo* sorbability, because a slight inflammatory response was reported in the case of the amorphous HAp

coating on silicone elastomer by pulsed laser deposition (Zabetakis et al., 1994).

HAp nanoparticles can be synthesized in a number of ways, such as wet chemical process (Jarcho et al., 1976; Schmidt, 2000; Cushing et al., 2004), sol–gel process (Masuda et al., 1990; Sanchez & Livage, 1990; Schmidt et al., 1998), and emulsion process (Lim et al., 1996; Sonoda et al., 2002). Among these processes, wet chemical process has been widely used because it is simple and the morphology of the HAp particles can be changed by reaction conditions such as pH, temperature and concentration of reactants or additives (Jarcho et al., 1976; Schmidt, 2000; Cushing et al., 2004). The morphology will affect the adsorption properties of biopolymers such as proteins and the ion-exchange property, because HAp belongs to a hexagonal crystal system and possesses different properties on its *a* and *c* planes (Kawasaki, 1991).

When low-crystallinity HAp nanoparticles synthesized via the above processes are calcined to increase thermal and chemical stability, the particles typically sinter into large agglomerates consisting of polycrystals (Barralet et al., 2000; Landi et al., 2000; Bernache-Assollant et al., 2003). Because sintered HAp polycrystals has poor dispersibility in liquid media and a large size distribution, it is difficult to control the surface morphology (covering ratio by HAp, surface roughness) of the above-mentioned inorganic/organic composite. Hydrothermal treatment of HAp particles in an aqueous medium under high pressure is known to enable the preparation of sintering-free HAp single crystals (Somiya et al., 1988; Yoshimura et al., 1994; Papargyris et al., 2002). However, this treatment generally leads to an increase in crystal size due to Ostwald ripening (Carless & Foster, 1966), and is restricted to laboratory-scale products as it is a high-pressure process.

In our previous article (Okada & Furuzono, 2006), in order to control the surface morphology of the above-mentioned composite, agglomerate-free HAp nanocrystals having a spherical morphology were fabricated by calcination with an anti-sintering agent surrounding the HAp particles and subsequent removal of the agent. That is, there was no contact among the particles during calcination. Original HAp nanoparticles with low crystallinity and a spherical morphology were prepared by a modified emulsion system (Sonoda et al., 2002) at 25°C, and calcined with calcium hydroxide [$Ca(OH)_2$]. $Ca(OH)_2$ was selected as the anti-sintering agent, because $Ca(OH)_2$ does not melt at the calcination temperature (800°C), presumably would not dissolve the HAp, and could be removed by washing with water after calcination.

In this article, original HAp particles having a rod-like morphology prepared by the wet chemical process were calcined with an anti-sintering agent in order to extend the application of calcination with an anti-sintering agent. Poly(acrylic acid) (PAA) was used to surround the HAp particles efficiently with the anti-sintering agent, and the thermal decomposition behavior of the agent during calcination was investigated. Furthermore, the influence of the anti-sintering agent on the crystal phase, composition, and particle size of the HAp crystals was investigated.

The HAp nanocrystals obtained here should be suitable for various applications, such as biomaterials, ion exchangers, adsorbents, catalysts, and dental and orthopedic ultrafine fillers for microporosity owing to their high dispersibility in liquid media and high thermal and chemical stability. Calcination with an anti-sintering agent has potential application to a wide range of calcined nanoceramic powders, such as alumina, titania, and magnesia, and offer significant benefits over existing technologies because the technique is simple, inexpensive, and amenable to scaling-up and processing.

Experimental

Materials

$Ca(OH)_2$ was prepared by the hydrolysis of calcium oxide obtained by calcination of alkaline-analysis-grade calcium carbonate ($CaCO_3$; Wako Pure Chemical Industries, Ltd., Osaka, Japan) at 1050°C for 3 h. A 25% ammonia solution and diammonium hydrogenphosphate [$(NH_4)_2HPO_4$] were purchased from Wako Pure Chemical Industries, Ltd. Guaranteed reagent-grade calcium nitrate tetrahydrate [$Ca(NO_3)_2{\cdot}4H_2O$] and ammonium nitrate [NH_4NO_3] were purchased from Nacalai Tesque Inc., Kyoto, Japan. PAA (weight-average molecular weight: 15,000), used as a

polymeric stabilizer, was purchased from Sigma-Aldrich Co., MO, USA. Milli-Q water with a specific resistance of 18.2×10^6 Ω cm was used (Millipore Corp., MA, USA).

HAp particles

Original HAp particles with a rod-like morphology were prepared by the wet chemical process as follows. 42 mM $Ca(NO_3)_2$ aq. and 100 mM $(NH_4)_2HPO_4$ aq. were prepared, and the pH of each solution was adjusted to 12.5 by adding a 25% ammonia solution. 800 ml of the $Ca(NO_3)_2$ aq. was poured into a 1-l reactor equipped with an inlet of N_2, a reflux condenser, and a half-moon type stirrer. After the temperature in the reactor had been raised to 80°C, 200 ml of the $(NH_4)_2HPO_4$ aq. was added into the reactor at a feeding rate of 20 m/h, and the resultant mixture was stirred for another 10 h at 80°C. The obtained HAp particles were centrifugally washed with water, and re-dispersed in a water medium.

Calcination

The calcination procedure of HAp particles with an anti-sintering agent is sketched in Figure 1. An amount of PAA, approximately equal in weight to the HAp particles, was dissolved in water at 1.0 wt%, and the pH of the PAA aq. was adjusted to 10.0. The PAA aq. was added in the HAp dispersion (solid content, 1.0 wt%), and the dipsersion was ultrasonicated for 5 min. A saturated $Ca(OH)_2$ aq. was added to the dispersion ($Ca(OH)_2$/COOH in PAA = 1/1 molar ratio) to precipitate poly(acrylic acid, calcium salt) (PAA-Ca) onto the HAp particles. The resultant HAp/PAA-Ca mixture was filtered, rinsed with water, and dried at 80°C for 2 h under reduced pressure. The dried HAp/PAA-Ca mixture was placed on an alumina tube in a horizontal furnace at room temperature in air. In order to calcine the mixture, the furnace was heated from room temperature to 800°C at a heating rate of 10°C/min, and the temperature was kept at 800°C for 1 h after the temperature had reached to 800°C. After that, the heater of the furnace was automatically turned-off. The resultant powder after calcination was centrifugally washed with 100 mM NH_4NO_3 aq. until the pH of the aqueous medium decreased to almost 7.0, and then washed with water three times. As a control procedure, the same original HAp particles were calcined without adding PAA and $Ca(OH)_2$.

Thermal decomposition of PAA-Ca

PAA-Ca was precipitated by adding a saturated $Ca(OH)_2$ aq. into PAA aq. at an initial pH of 10.0 in the absence of HAp particles. The precipitation

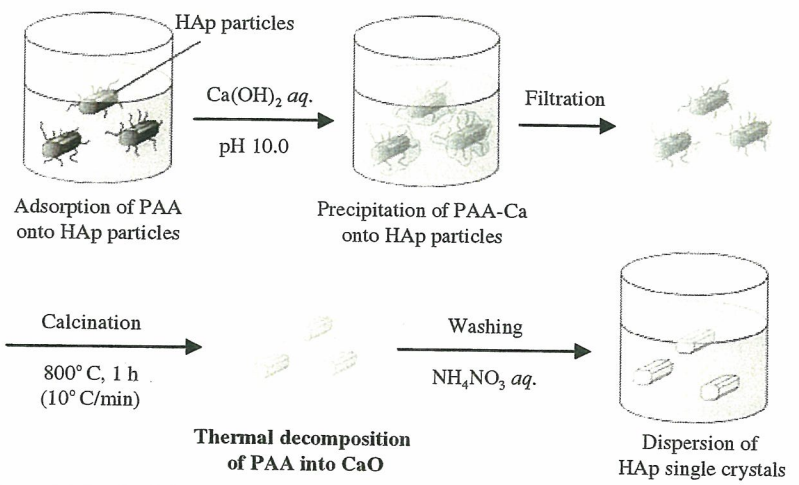

Figure 1. Schematic model for the fabrication of single nanocrystals of hydroxyapatite calcined with an anti-sintering agent and subsequently removing the agent.

was filtered, rinsed with water, and dried at 80°C for 2 h under reduced pressure. The PAA-Ca was calcined at 800°C for 1 h with the same procedure described in the Section 'Calcination'. The thermal decomposition behavior of PAA-Ca was measured by a thermogravimeter (TG; EXSTAR6000 TG/DTA6300, Seiko Instruments Inc., Chiba, Japan). The heating rate for TG measurement was 10°C/min and the temperature range was from 30°C to 1000°C.

Measurements

Identification of the product was conducted by X-ray diffraction (XRD) measurement (RAD-X; Rigaku International Co., Tokyo, Japan) with CuKa radiation, and diffuse reflectance Fourier-transform infrared (FT-IR) spectroscopy (Spectrum One; Perkin–Elmer Inc., MA, USA). The morphology of the HAp crystals was observed by scanning electron microscopy (SEM; JSM-6301F, JEOL Ltd., Tokyo, Japan) and transmission electron microscopy (TEM; JEM-2000 EXII, JEOL Ltd.). The size distribution of the HAp crystals dispersed in an ethanol medium was measured at a 10-ppm concentration by dynamic light scattering (DLS; ELS-8000, Otsuka Electronics Co., Ltd., Kyoto, Japan) at a light-scattering angle of 90°. The Ca/P atomic ratio of each HAp was measured by inductively coupled plasma-atomic emission spectrometry (ICP-AES; SPS4000, Seiko Instrument Inc., Chiba, Japan). Calcium and phosphorus standard solutions for ICP-AES were purchased from Kanto Chemical Co., Inc., Tokyo, Japan. The specific surface area of the particles was measured by the Brunauer–Emmett–Teller (BET) triple-point method with nitrogen adsorption (NOVA1200e, Quantachrome Instruments, FL, USA) after degassing the powder at 100°C under reduced pressure for 10 min. The data resulting from BET measurements are presented as means ± SD for mean (N = 3). Statistical comparisons were performed with the use of a Student's t-test. The level of statistical significance was defined as $p < 0.01$.

Results and discussion

First, in order to check the thermal decomposition behavior of PAA-Ca used as an anti-sintering agent, PAA-Ca was calcined in air at 800°C for 1 h. Figure 2 shows the FT-IR spectra of PAA and PAA-Ca. PAA showed major peaks at 1695 cm^{-1}, corresponding to the C=O stretching of the carboxyl groups and at 1453/1415 cm^{-1}, corresponding to the CH_2 and CH bending mode of the PAA chain (Figure 2a). In the spectrum of the PAA-Ca shown in Figure 2b, the peak at 1695 cm^{-1} decreased and a new peak appeared at 1565/1330 cm^{-1}, corresponding to the stretching mode of ionized carboxyl groups, suggesting the formation of a significant number of Ca–O interactions (Sindhu & Valiyaveettil, 2004). The broad peak around 3600 cm^{-1} in Figure 2b seems to be corresponding to the OH stretching in free COOH or absorbed water, because $Ca(OH)_2$ crystal phase was not observed by XRD. After calcination of PAA-Ca (Figure 2c), new characteristic peaks appeared at 3644 cm^{-1} corresponding to the OH stretching in $Ca(OH)_2$. This indicates that the organic component of PAA-Ca was completely decomposed and PAA-Ca became $Ca(OH)_2$ after calcination. It should be noted that the formation of $Ca(OH)_2$ is favorable because it can be removed by dissolving in an aqueous medium.

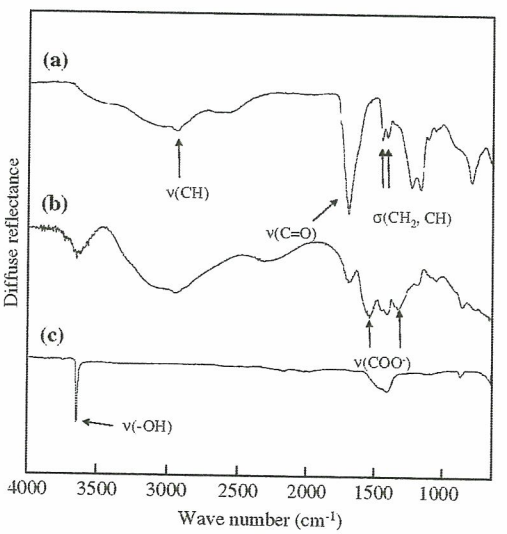

Figure 2. FT-IR spectra of (a) poly(acrylic acid) (PAA); (b) poly(acrylic acid calcium salt) (PAA-Ca) precipitated by adding a saturated $Ca(OH)_2$ aq. in a PAA aqueous solution ($Ca(OH)_2$/COOH in PAA = 1/1 molar ratio); (c) PAA-Ca after calcination at 800°C for 1 h at a heating rate of 10°C/min.

The *in situ* thermal decomposition of PAA-Ca during calcination was measured by TG as shown in Figure 3. The TG measurement was conducted at a heating rate of 10°C/min in air. In the case of $CaCO_3$ with a calcite structure (Figure 3a), the weight loss started at 707°C and its weight decreased by 44.2%, which should be due to the detachment of CO_2 molecules (43.9% in weight, calculated from the chemical formula of $CaCO_3$). On the other hand, the weight of PAA-Ca gradually decreased to 87.2% due to the evaporation of absorbed water, and drastically decreased at 516°C to 49.6% with exothermic heat (see Figure 3b: time vs. temperature). This indicates the thermal decomposition of the organic components in PAA-Ca. Another weight loss started at 683°C and 28.1% of its weight remained in the latter stage. The weight loss $[(49.6-28.1)/49.6\times100 = 43.3\%]$ and the starting temperature (683°C) of the latter stage almost corresponded to those of $CaCO_3$ (weight loss, 44.2%; temperature, 707°C). These results indicate that PAA-Ca was decomposed finally into CaO with the detachment of CO_2 molecules during calcination, and $Ca(OH)_2$ observed in Figure 2c was formed by a hydrolysis reaction of a part of CaO with moisture in air, as described in the following equation:

$$\text{PAA-Ca} \overset{520^{\circ}\text{C}\sim}{\rightarrow} CaCO_3 \overset{680^{\circ}\text{C}\sim}{\rightarrow} CaO \overset{+H_2O}{\rightarrow} Ca(OH)_2 \quad (1)$$

The rod-like HAp particles prepared by the wet chemical process were calcined with PAA-Ca surrounding the particles (Figure 1). In order to surround the particles with PAA-Ca, first, PAA was adsorbed on the surfaces of the HAp particles in an aqueous medium. PAA can adsorb on the HAp surfaces (Misra, 1993; Yoshida et al., 2001; Bonapasta et al., 2001), and thus act as a polymeric dispersant to prevent flocculation in an aqueous medium. The addition of calcium ions into an aqueous PAA solution induces precipitation of PAA-Ca. Accordingly, when calcium ions are added to the PAA-stabilized HAp dispersion, PAA-Ca precipitates onto the surfaces of the HAp particles. The PAA-Ca presumably acts as an anti-sintering agent, because there is no contact among the HAp particles by surrounding them with PAA-Ca and/or its thermally decomposed product, CaO, during calcination.

In order to investigate the effect of the anti-sintering agent on the crystal phase and composition of HAp, XRD and FT-IR measurements were conducted. The results are shown in Figures 4 and 5. In Figure 4, both the XRD profiles of the particles calcined without additives and those with PAA-Ca showed highly crystalline HAp. It is worth pointing out that other calcium phosphate phases, CaO, and $Ca(OH)_2$ could not be detected from each XRD profile. In the FT-IR spectra shown in Figure 5, the absorption bands at

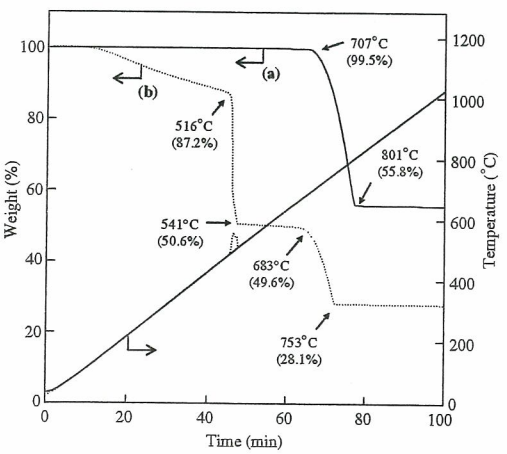

Figure 3. Thermal decomposition behavior of (a; solid line) $CaCO_3$ with calcite structure and (b; dotted line) PAA-Ca at a heating rate of 10°C/min in air.

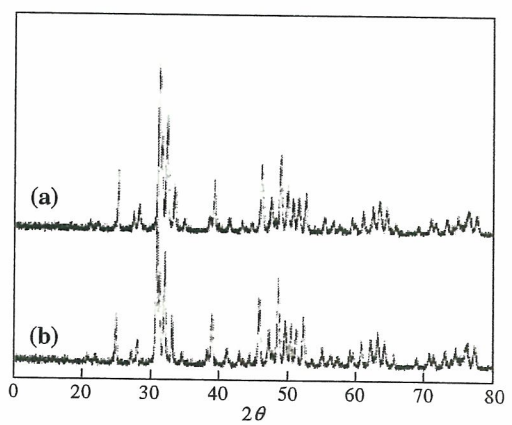

Figure 4. XRD patterns of HAp nanocrystals calcinated (a) without additive and (b) with PAA-Ca at 800°C for 1 h at a heating rate of 10°C/min in air, followed by washing with water.

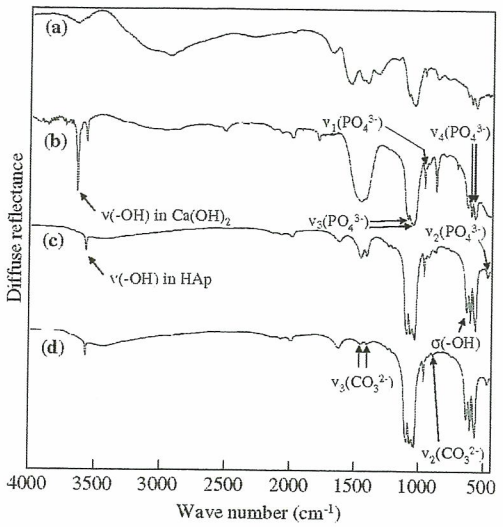

Figure 5. FT-IR spectra of (a) a mixture of HAp particles and PAA-Ca prepared by addition of saturated $Ca(OH)_2$ aq. in PAA-stabilized HAp aqueous dispersion, (b) the HAp/PAA-Ca mixture after calcination at 800°C for 1 h, (c) HAp nanocrystals after washing with water, and (d) HAp crystals after calcination without additives.

603/572 and 474 cm^{-1} are, respectively attributed to $\nu_4PO_4^{3-}$ and $\nu_2PO_4^{3-}$ in crystalline HAp. Absorptions at 1092/1045 and 963 cm^{-1} are, respectively attributed to $\nu_3PO_4^{3-}$ and $\nu_1PO_4^{3-}$. The sharp absorptions of OH stretching and vibration at 3573 and 632 cm^{-1} indicate that the material exhibits high crystallinity (Fowler, 1974; Taylor et al., 2001) after the calcination (Figure 5b–d). In the FT-IR spectrum of the HAp calcined with PAA-Ca followed by washing with water (Figure 5c), a peak at 3644 cm^{-1} due to the stretching of OH in $Ca(OH)_2$ (observed in Figure 5b) disappeared, suggesting removal of $Ca(OH)_2$. Bands at 1456/1413 and 877 cm^{-1}, attributed to CO_3^{2-} substituting phosphate positions in the HAp lattice (Emerson & Fisher, 1962), increased in the case of calcination with PAA-Ca (Figure 5c) as compared to that without additives (Figure 5d). This seems to be due to incorporation of CO_3^{2-} in HAp lattice by the reaction with atmospheric carbon dioxide generated by thermal decomposition of PAA-Ca during calcination. CO_3^{2-} in Figure 5d seems to be incorporated during the wet chemical process and the reaction with CO_2 in air during calcination (Ishikawa et al.,

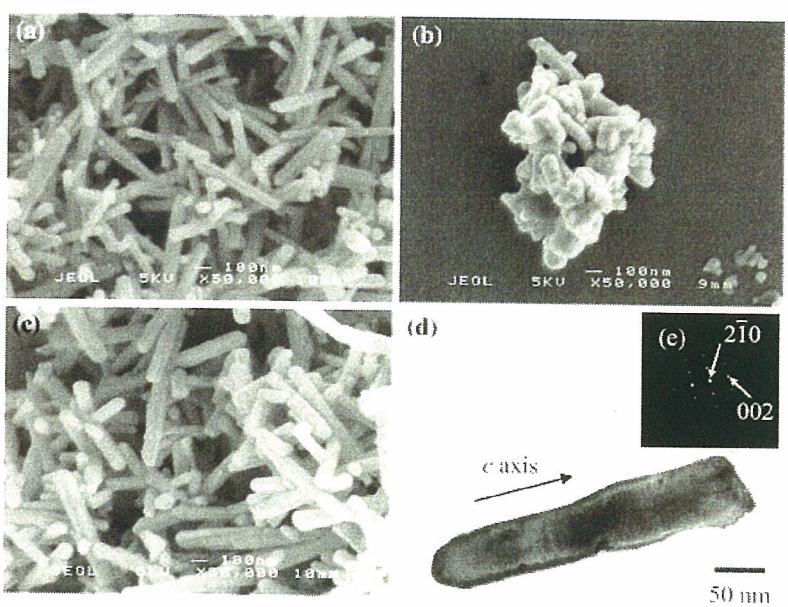

Figure 6. SEM photographs of (a) original HAp particles before calcination, and HAp crystals after calcination (b) without additive and (c) with PAA-Ca. (d) A TEM photograph and (e) the associated electron diffraction pattern of a HAp crystal calcined with PAA-Ca, showing the crystal consisting of a single HAp phase.